THE JOURNAL OF BIOLOGICAL CHEMISTRY
Vol. 278, No. 49, Issue of December 5, pp. 49031–49043, 2003
Printed in U.S.A.

Tuba, a Novel Protein Containing Bin/Amphiphysin/Rvs and Dbl Homology Domains, Links Dynamin to Regulation of the Actin Cytoskeleton*

Received for publication, July 25, 2003, and in revised form, September 16, 2003
Published, JBC Papers in Press, September 22, 2003, DOI 10.1074/jbc.M308104200

Marco A. Salazar‡§¶, Adam V. Kwiatkowski§‖, Lorenzo Pellegrini‡ ‡‡, Gianluca Cestra‡ ‡‡, Margaret H. Butler‡, Kent L. Rossman§§, Daniel M. Serna‖, John Sondek§§, Frank B. Gertler‖, and Pietro De Camilli‡¶¶**

From the ‡Department of Cell Biology and the Howard Hughes Medical Institute, Yale University School of Medicine, New Haven, Connecticut 06519, the ‖Department of Biology, Massachusetts Institute of Technology, Cambridge, Massachusetts 01239, and the §§Department of Biophysics and Biochemistry and the Lineberger Cancer Center, University of North Carolina, Chapel Hill, North Carolina 27599

Tuba is a novel scaffold protein that functions to bring together dynamin with actin regulatory proteins. It is concentrated at synapses in brain and binds dynamin selectively through four N-terminal Src homology-3 (SH3) domains. Tuba binds a variety of actin regulatory proteins, including N-WASP, CR16, WAVE1, WIRE, PIR121, NAP1, and Ena/VASP proteins, via a C-terminal SH3 domain. Direct binding partners include N-WASP and Ena/VASP proteins. Forced targeting of the C-terminal SH3 domain to the mitochondrial surface can promote accumulation of F-actin around mitochondria. A Dbl homology domain present in the middle of Tuba upstream of a Bin/amphiphysin/Rvs (BAR) domain activates Cdc42, but not Rac and Rho, and may thus cooperate with the C terminus of the protein in regulating actin assembly. The BAR domain, a lipid-binding module, may functionally replace the pleckstrin homology domain that typically follows a Dbl homology domain. The properties of Tuba provide new evidence for a close functional link between dynamin, Rho GTPase signaling, and the actin cytoskeleton.

Fission of clathrin-coated and other endocytic vesicles from the plasma membrane involves the cooperation of several membrane-associated proteins, among which the GTPase dynamin plays a key role (1, 2). The participation of dynamin in the fission of endocytic vesicles has been established by a variety of experimental approaches in *Drosophila*, cultured cells, and cell-free systems, although the precise mechanism of fission and the role of dynamin in this reaction remain unclear (3).

Several dynamin partners thought to participate in dynamin recruitment or function have been identified (3, 4). At the synapse, where endocytosis plays a key role in the recycling of synaptic vesicle membranes, two prominent dynamin partners are amphiphysin and endophilin (5–7). Amphiphysin has a three-domain structure with an evolutionarily conserved N-terminal module of ~250 amino acids called the Bin/amphiphysin/Rvs (BAR)[1] domain, a variable central region, and a C-terminal Src homology-3 (SH3) domain that binds dynamin. Endophilin has a similar domain structure (2). Although the N-terminal domain of endophilin is substantially divergent in amino acid composition from the BAR domain of amphiphysin, it shares some similarity at critical sites, leading to its classification as a BAR domain (8).[2] Accordingly, the BAR domains of amphiphysin and endophilin share functional similarities because they both can bind and deform lipid bilayers and mediate homo- and heterodimerization (6, 8–10). Dynamin also can bind and deform lipid bilayers, and it has been proposed that endophilin and amphiphysin might help to recruit and possibly assist dynamin in the generation of membrane curvature at endocytic pits (8, 10).

The closest homologue of amphiphysin and endophilin in *Saccharomyces cerevisiae* is Rvs167, that forms a stable heterodimer with Rsv161; Rvs167 has a domain structure like amphiphysin, whereas Rvs161 (homologous to the mammalian protein Bin3) possesses only a BAR domain. Mutation of either one or both components of this heterodimer in yeast produces defects in endocytosis and actin function (11). Such a dual phenotype is typical of most mutations in actin regulatory and endocytosis genes in yeast (12). These observations, together with results from a variety of studies in mammalian cells, have suggested a link between endocytosis and actin, although such a link has remained mechanistically elusive (13, 14). Foci of actin can often be seen at endocytic sites (15), and endocytic vesicles with actin tails have also been observed (16). Interest-

* This work was supported in part by National Institutes of Health Grants NS36251 and CA46128 and United States Army Medical Research and Development Command Grant DAMD17-97-7068) (to P. D. C.); by National Institutes of Health Grant GM58801, a W. M. Keck Distinguished Young Scholar Award, and a McKnight Scholar Award (to F. B. G.); and by National Institutes of Health Grant GM62299 (to J. S.). The costs of publication of this article were defrayed in part by the payment of page charges. This article must therefore be hereby marked "*advertisement*" in accordance with 18 U.S.C. Section 1734 solely to indicate this fact.

The nucleotide sequence(s) reported in this paper has been submitted to the GenBank™/EBI Data Bank with accession number(s) AY196211 and AY383729.

§ Both authors contributed equally to this work.

¶ Supported by a research supplement for underrepresented minorities from NCI, National Institutes of Health.

** Supported by an Anna Fuller predoctoral fellowship.

‡‡ Supported by a fellowship from Telethon (Italy).

¶¶ To whom correspondence should be addressed: Dept. of Cell Biology and Howard Hughes Medical Inst., Yale University School of Medicine, 295 Congress Ave., BCMM 236, New Haven, CT 06519. Tel.: 203-737-4461; Fax: 203-737-4436; E-mail: pietro.decamilli@yale.edu.

[1] The abbreviations used are: BAR, Bin/amphiphysin/Rvs; SH3, Src homology-3; DH, Dbl homology; PH, pleckstrin homology; HA, hemagglutinin; GST, glutathione *S*-transferase; RACE, rapid amplification of cDNA ends; mant-, *N*-methylanthraniloyl-; MALDI-TOF, matrix-assisted laser desorption ionization time-of-flight; EGFP, enhanced green fluorescent protein.

[2] See smart.embl-heidelberg.de/smart/get_members.pl?WHAT=NRDB_COUNT&NAME=BAR.

ingly, these actin tails contain both dynamin and dynamin-interacting proteins (17, 18).

Several binding partners of dynamin are either physically or functionally linked to actin or actin regulatory proteins. These include, among others, syndapin/pacsin and intersectin/DAP160 (13, 14). Intersectin, in particular, represents a striking example of a multidomain protein that links dynamin to proteins that directly or indirectly control actin polymerization, such as the phosphatidylinositol-4,5-bisphosphate phosphatase, synaptojanin, N-WASP (neuronal Wiskott-Aldrich syndrome protein), and the Rho family GTPase Cdc42 (19, 20). N-WASP is a member of the WASP superfamily of proteins that includes SCAR/WAVE. All members of this family possess a conserved C terminus that can bind to and activate the Arp2/3 complex, a collection of proteins that catalyzes the nucleation of actin filaments (21). N-WASP exists predominantly in an autoinhibited state. When activated Cdc42 or the adaptor protein Nck binds to N-WASP, this autoinhibition is relieved. Phosphatidylinositol 4,5-bisphosphate can further activate N-WASP in combination with Cdc42 and Nck (22–24). Intersectin functions to bring together N-WASP and, through the guanyl nucleotide exchange activity of its Dbl homology (DH) domain, activated GTP-bound Cdc42, thus activating Arp2/3 and promoting actin nucleation (19). The endocytic protein syndapin/pacsin, which, like intersectin, binds both dynamin and N-WASP, can promote N-WASP-dependent actin nucleation (25). Thus, intersectin and syndapin function as molecular links between endocytosis and actin assembly.

The Arp2/3 complex plays a key role in generating actin-based protrusive forces that can drive the movement of vesicles and intracellular pathogens such as *Listeria monocytogenes* (26). Members of the Ena (Enabled)/VASP (vaodilator-stimulated phosphoprotein) protein family (Mena (mammalian Enabled), VASP, and EVL (Ena-VASP-like)) greatly accelerate the actin-based movement of *Listeria* (27, 28). Ena/VASP proteins are concentrated in the tips of filopodia and lamellipodia and are known to regulate actin filament geometry in protruding lamellipodia (29, 30). At a molecular level, Ena/VASP proteins are thought to antagonize the activity of capping proteins, thereby permitting increased actin filament elongation at barbed ends and decreasing the density of branched structures by an unknown mechanism (29, 31).

A search of protein data bases for BAR domains reveals a large number of BAR domain-containing proteins in a variety of animal and plant species. In most of these proteins, which generally contain a C-terminal SH3 domain, the BAR domain is located in the N terminus. However, in three homologous vertebrate sequences, the BAR domain is not located at the N terminus, but is instead found downstream of a DH domain. Most DH modules characterized thus far are located upstream of a pleckstrin homology (PH) domain, and the lipid-binding properties of the PH domain are thought to play a critical role in the localization and regulation of DH domain activity (32). We have characterized one of these three proteins, which we have named Tuba. In an independent line of study, we identified the mouse homolog of Tuba in a yeast two-hybrid screen using the Ena/VASP protein EVL as bait. Collectively, our study demonstrates that Tuba is a large scaffold protein that binds dynamin and a variety of actin regulatory proteins and that activates Cdc42. Our results suggest that Tuba functions as in important link between dynamin function, Rho GTPase signaling, and actin dynamics regulated by WASP/WAVE superfamily and Ena/VASP proteins.

EXPERIMENTAL PROCEDURES

Antibodies and Reagents—The following antibodies were used in this study: rat anti-hemagglutinin (HA) monoclonal epitope (clone 3F10, Roche Applied Science), anti-dynamin polyclonal antibody DG1 (our laboratory) and monoclonal antibody Hudy-1 (Upstate Biotechnology, Inc.), anti-amphiphysin-1 monoclonal antibody-3 (33) and anti-N-WASP polyclonal antibody (gifts of P. Aspenstrom (Ludvig Institute for Cancer Research, Uppsala, Sweden) and M. W. Kirschner (Harvard Medical School)), anti-CR16 polyclonal antibody (gift of H. Y. Ho and M. W. Kirschner), anti-WAVE1 polyclonal antibody (gift of John Scott, Vollum Institute), anti-Mena monoclonal antibody (our laboratory), anti-green fluorescent protein polyclonal antibody (Clontech), anti-actin monoclonal antibody (Sigma), anti-synaptotagmin monoclonal antibody (gift of Reinhard Jahn, Max-Planck Institute for Biological Chemistry, Göttingen, Germany), and anti-GM-130 antibody (Graham Warren, Yale University). Anti-Tuba polyclonal antibodies were generated by injecting rabbits with a glutathione *S*-transferase (GST) fusion protein encompassing the final 292 amino acids of human Tuba. The antibodies were affinity-purified on the antigen coupled to SulfoLink beads (Pierce) according to the manufacturer's instructions. A GST fusion protein of the PH domain of phospholipase Cδ was kind gift of Antonella De Matteis (Consorzio Mario Negri Sud, Italy). A GST fusion protein of the BAR domain of amphiphysin-1 was described previously (10). The KIAA1010 clone was obtained from the Kazusa Institute.

5′-Rapid Amplification of cDNA Ends (RACE)—To obtain the full-length sequence of Tuba from the KIAA1010 clone, human skeletal muscle Marathon-Ready cDNAs (Clontech) were utilized for 5′-RACE using KIAA1010-specific primers and the Advantage 2 PCR enzyme system (Clontech). Based on this sequence, a full-length clone was generated by PCR using probes corresponding to the 5′- and 3′-ends of the Tuba sequence and human brain Marathon-Ready cDNAs (Clontech) as a template. Nucleotide sequencing confirmed the sequences of KIAA1010 and of the N-terminal region of the protein obtained by 5′-RACE with the exception of the absence in KIAA1010 of 40 amino acids in the second half of the BAR domain (see Fig. 1*A*). Multiple clones generated by PCR in different amplification cycles yielded only sequences including the 40 amino acids. The nucleotide sequence of human Tuba has been deposited in the GenBank™/EBI Data Bank under accession number AY196211.

Yeast Two-hybrid Screen—Full-length EVL was used as bait in the LexA two-hybrid system (Clontech) to probe an embryonic day 19 mouse library. Two independent clones of Tuba comprising amino acids 1502–1577 and 1092–1577 (see Fig. 1*A*) were identified as strong interactors. Full-length murine Tuba was constructed by ligating the larger of the two clones with fragments generated by reverse transcription-PCR using Tuba-specific primers and a mouse cDNA library. The nucleotide sequence of mouse Tuba has been deposited in the GenBank™/EBI Data Bank under accession number AY383729.

Affinity Chromatography—GST or GST fusion proteins of SH3 domain-containing regions of Tuba were bound to glutathione beads (Amersham Biosciences) and incubated with a Triton X-100-solubilized rat brain extract. Bound material was recovered by centrifugation, followed by elution with SDS and separation by SDS-PAGE.

For biochemical analysis of the interaction of the SH3-6 domain of Tuba with actin regulatory proteins in non-neuronal cell extracts, D7 fibroblastic cells, which lack endogenous expression of all Ena/VASP proteins, were used (34). Uninfected or infected D7 cells were grown to confluency and extracted in Nonidet P-40 lysis buffer. Cell extracts were clarified by centrifugation and used for affinity chromatography experiments as described above. 10–15 μg of GST or GST fusion protein was incubated with 1 mg of lysate.

Immunocytochemistry of Brain Tissue—Immunofluorescence of frozen rat brain sections was performed by standard procedures on formaldehyde-perfused brains. Anti-Tuba immunogold labeling was performed on lysed synaptosomes embedded in agarose, followed by Epon embedding and thin sectioning as described (35).

Guanine Nucleotide Exchange Assays—Exchange assays using bacterially expressed and purified Rho GTPases were performed essentially as described (36). In particular, 2 μM RhoA(C190S), Rac1(C188S), or Cdc42(C188S) was added to buffer containing 20 mM Tris (pH 7.5), 100 mM NaCl, 5 mM $MgCl_2$, 1 mM dithiothreitol, 10% glycerol, and 400 nM mant-GTP (Molecular Probes, Inc.) and allowed to equilibrate for 5 min before adding the indicated concentrations of His-tagged Tuba DH domain or 200 nM His-tagged Vav2 DH-PH fragment. Increased fluorescence indicative of mant-GTP binding to GTPases was monitored using a PerkinElmer LS-55 spectrophotometer (λ_{ex} = 360 nm and λ_{em} = 440 nm, slits = 5/5 nm) thermostatted to 25 °C. Fluorescence was normalized to the initial value at the start of the experiment. A fragment containing the DH and BAR domains of Tuba is insoluble upon expression in *Escherichia coli*, preventing a comparison of exchange rates between this larger portion of Tuba and the isolated DH domain of Tuba.

Transferrin Uptake—Chinese hamster ovary cells were transfected with pcHA (pcDNA3-based vector)-full-length Tuba or pcHA-Tuba SH3-1,2,3,4 using FuGENE 6 transfection reagent (Roche Applied Science) and incubated overnight. They were then washed with serum-free medium and incubated in serum-free medium for 24 h in the presence of Alexa-transferrin (Molecular Probes, Inc.) during the last 7 min before a brief wash with phosphate-buffered saline, followed by fixation with 4% formaldehyde. Cells were stained by immunofluorescence according to standard procedures.

Peptide Binding—Overlapping SPOTs peptides corresponding to the proline-rich regions of mouse N-WASP (amino acids 217–399), SCAR/WAVE1 (amino acids 274–402), EVL (amino acids 157–210), and Mena (amino acids 277–351) were custom-synthesized by Sigma. All peptides are 12-mers offset by three amino acids, and each spot carries an equivalent amount of peptide (5 nmol) covalently attached to the membrane. A negative control peptide was added (no. 118 on the blot) that contains a known proline-rich binding site for Ena/VASP proteins that does not bind SH3 domains. The Tuba SH3-6 domain in pGEX-2TK was labeled by phosphorylating with protein kinase A and [γ-^{32}P]ATP. The relative intensity of each spot was calculated by converting the PhosphorImager scan into an 8-bit image and measuring the average pixel intensity in a 74-pixel circle centered over each spot in Scion Image. This value was then divided by the background (the average intensity value of the 10 lowest spots) for comparison.

Mitochondrial Targeting of the Tuba SH3-6 Domain—The mouse Tuba SH3-6 domain was fused in-frame to a modified retroviral expression vector downstream of an ATG start codon and upstream of a fusion between DsRed2 and the mitochondrial targeting sequence from the *L. monocytogenes* protein ActA (excluding Ena/VASP-binding regions) (37). This construct, referred to as SH3-6-mito, was used to transiently transfect CAD cells. Cells were plated onto poly-D-lysine-coated coverslips 24 h post-transfection. The medium was replaced with serum-free medium to induce differentiation 3–4 h after plating. Cells were incubated for an additional 24–36 h before fixation with 4% formaldehyde. Previously established procedures were used to visualize cells by immunofluorescence.

Miscellaneous—We carried out Western and Northern blotting following standard procedures. For Northern blotting, human multiple-tissue RNA blots were obtained from Clontech. For multiple-tissue Western blotting, tissues were isolated and prepared as described previously (38). Far-Western assays and gel overlays were carried out using standard procedures. Immunoprecipitations were carried out as described previously (38).

RESULTS

Tuba Is a Novel BAR Domain-containing Protein—A BLAST search for proteins containing a domain related to the BAR domain of amphiphysin-1 revealed a large number of sequences. In one (KIAA1010), the putative BAR domain is not located at the N terminus of the protein as in most other sequences, but downstream of a DH domain (Fig. 1*A*). Although the overall homology to the amphiphysin-1 BAR domain is limited (24% identical and 39% similar) (Fig. 1*B*), similarities are concentrated in regions generally conserved among the Bin/amphiphysin family. This region in KIAA1010 is currently identified as a BAR domain by protein module-recognizing algorithms such as those of the Pfam and SMART programs.

We undertook 5′-RACE using human cDNAs from muscle and brain to isolate a full-length protein corresponding to KIAA1010. This protein, which we have named Tuba in line with the tradition of naming large synaptic proteins after musical instruments (39), comprises 1577 amino acids with a predicted molecular mass of 178 kDa. The corresponding gene is located on human chromosome 10. The domain structure of Tuba (Fig. 1*A*) includes four N-terminal SH3 domains (referred to as SH3-1, SH3-2, SH3-3, and SH3-4), a predicted coiled-coil domain, a DH domain, the BAR domain, and two additional C-terminal SH3 domains (SH3-5 and SH3-6). In addition, a proline-rich low complexity region containing putative SH3 domain-binding sites is present upstream of the coiled-coil region (Fig. 1*A*).

In an independent line of study, a yeast two-hybrid screen aimed at identifying ligands for the Ena/VASP family protein EVL from an embryonic mouse library led to the isolation of two independent clones highly homologous to the C terminus of KIAA1010 (Fig. 1*A*) (data not shown). Reverse transcription-PCR using an embryonic mouse cDNA library was carried out to obtain the full-length gene, which turned out to be the mouse ortholog of Tuba. Mouse Tuba is 70% identical and 77% similar to human Tuba, has a similar domain structure, and is encoded by a gene located on mouse chromosome 19.

Searches through genomic and expressed sequence tag data bases revealed numerous expressed sequence tags to two genes that encode proteins homologous to the C-terminal half of Tuba in both human and mouse. We have named these proteins Tuba2 and Tuba3 (Fig. 1*A*). Tuba2 is located on human chromosome 4 and mouse chromosome 3, and Tuba3 is located on human chromosome 5 and mouse chromosome 8. Tuba2 is 41% identical and 60% similar to Tuba, and Tuba3 is 25% identical and 41% similar to Tuba. Tuba2 is 31% identical and 48% similar to Tuba3. Recent searches have also revealed what appears to be an alternately spliced form of Tuba that is similar in structure to Tuba2 and Tuba3 (Fig. 1*A*).

A putative ortholog of Tuba, GEI-18 (GEX interactor-18), was identified in *Caenorhabditis elegans* (Fig. 1*A*) (40). Two alternate transcripts of GEI-18 are described that comprise the N- and C-terminal halves of the protein. Although not recognized by Pfam or SMART, the region C-terminal of the DH domain in GEI-18 appears to be very similar to a BAR domain. A comparison of the BAR domains of the Tuba family of proteins with each other and human amphiphysin-1 is shown in Fig. 1*B*.

Tuba Is Ubiquitous—Northern blot analysis of human tissues with a probe corresponding to the C terminus of Tuba (nucleotides 4035–4540) revealed two transcripts of 7.3 and 6 kb (Fig. 2*A*) whose levels varied in different tissues. A probe directed against the N-terminal half of the protein (nucleotides 1246–1696) recognized only the larger transcript (data not shown). A third transcript of 4.5 kb was observed in a number of mouse tissues with a larger probe corresponding to the C terminus of mouse Tuba (nucleotides 2971–4742) (data not shown). This Tuba mRNA likely encodes only the second half of the protein, *i.e.* a Tuba splice variant similar in domain structure to the homologous proteins Tuba2 and Tuba3 (Fig. 1*A*). When tested by Western blotting against various rat tissues, affinity-purified antibodies generated against the C terminus of Tuba recognized a band at the expected molecular mass of full-length Tuba (~180 kDa). The band was the strongest in testis, followed by brain, heart, liver, spleen, and lung. In addition, the same antibodies recognized lower molecular mass bands at ~105 and 75 kDa with differential tissue distribution that may represent alternatively spliced forms of Tuba or proteolytic C-terminal fragments (Fig. 2*B*). The 75-kDa band may also represent cross-reactivity of the antibodies against either Tuba2 or Tuba3, whose molecular masses are predicted to be in this range. Collectively, these data indicate that Tuba has a broad tissue distribution and may exist in multiple isoforms.

Tuba Is Found at the Synapse—To determine the localization of Tuba in brain, where dynamin participates in the clathrin-mediated endocytosis of synaptic vesicles, rat brain cryosections were stained for Tuba by immunofluorescence. Tuba immunostaining yielded a punctate pattern outlining the surface of neuronal perikarya and dendrites that co-localized with immunoreactivity for the synaptic markers amphiphysin-1 and dynamin-1 (Hudy-1 antibodies) (Fig. 3*A*). In addition, Tuba immunoreactivity was observed within neuronal cell bodies at locations that corresponded to the Golgi complex, as shown by counterstaining for the Golgi marker GM-130 (41). However, high magnification observation indicated that GM-130 and

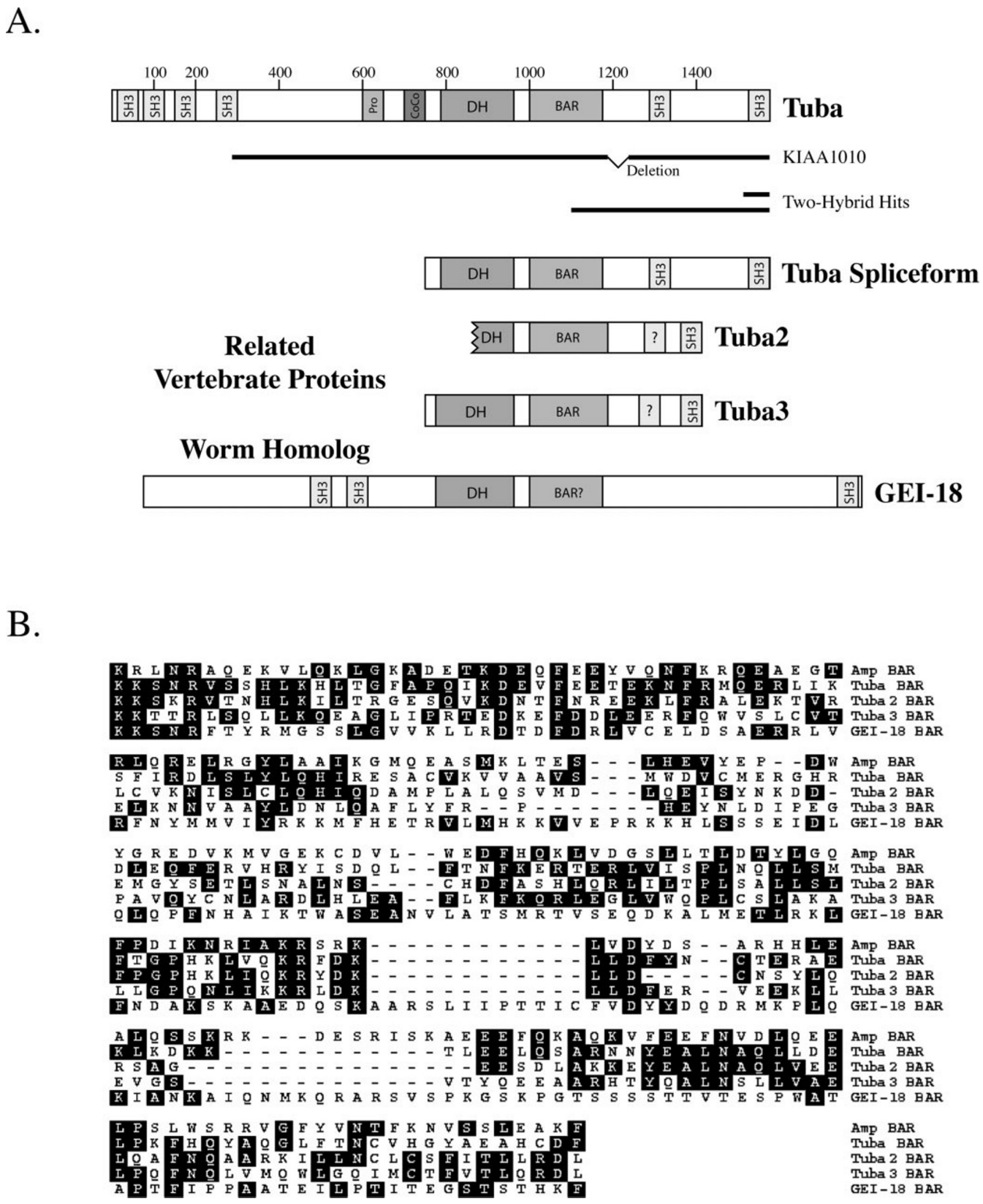

FIG. 1. **Domain structure of Tuba and related proteins.** *A*, Tuba, Tuba2, and Tuba3 are shown with domains of interest noted. The *thick lines* below Tuba indicate the portion of Tuba encoded by KIAA1010 and the partial clones isolated in the yeast two-hybrid screen for EVL interactors. Also shown is the shorter isoform of Tuba as well as the *C. elegans* Tuba homolog, GEI-18. *B*, shown is an alignment of the BAR domains of the Tuba family of proteins. The amphiphysin (*Amp*), Tuba, and Tuba3 BAR domains are from human; the Tuba2 sequence is from monkey; and the GEI-18 sequence is from *C. elegans*.

Tuba did not have an overlapping distribution, suggesting that the two antigens localized to distinct Golgi complex subcompartments (Fig. 3*A*).

To analyze the synaptic localization of Tuba in more detail, lysed synaptosomes were processed for anti-Tuba immunogold electron microscopy using a pre-plastic embedding procedure.

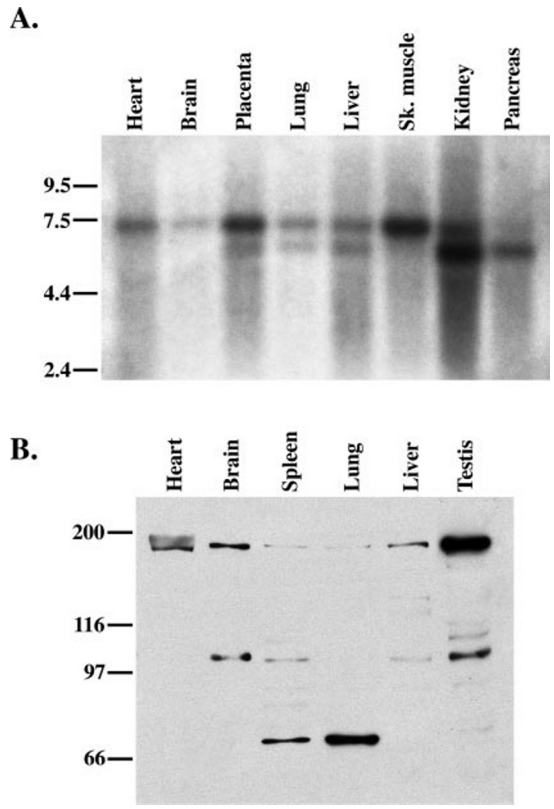

FIG. 2. **Ubiquitous expression of Tuba transcripts and their protein products.** *A*, multiple-tissue Northern blot using a probe directed against the 3′-end of Tuba. *B*, multiple-tissue Western blot of rat tissue post-nuclear supernatants with affinity-purified Tuba-specific antibodies. *Sk.*, skeletal.

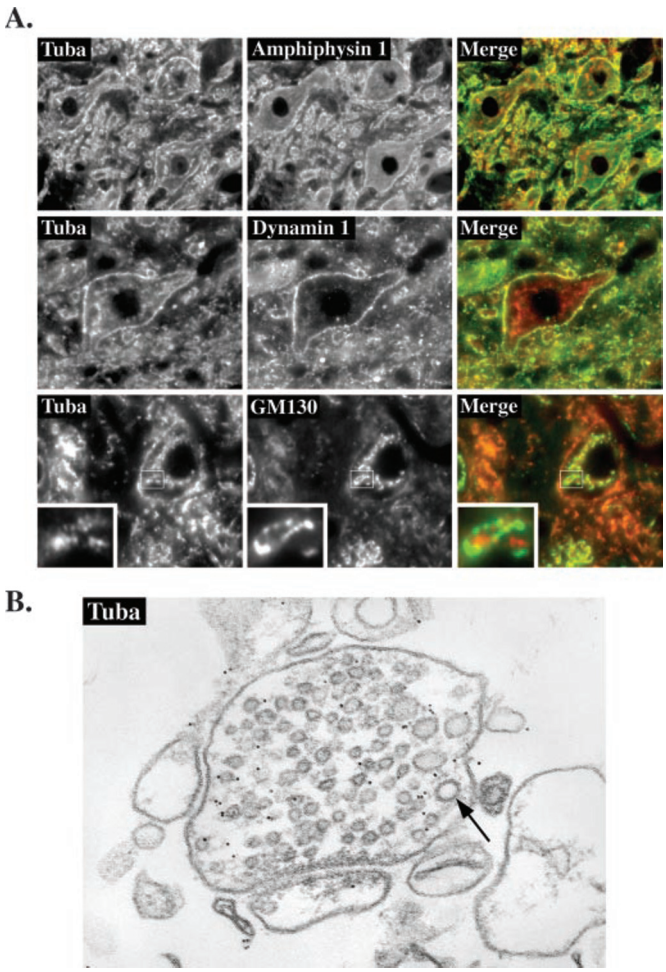

FIG. 3. **Tuba is concentrated at the synapse in brain.** *A*, double immunofluorescence of rat brainstem frozen sections with antibodies directed against Tuba (*red*) and other antigens (*green*) as indicated. Tuba co-localizes with the synaptically enriched proteins amphiphysin-1 and dynamin-1. Synapses appear as bright fluorescent puncta that outline the surface of perikarya and dendrites. In addition, Tuba immunoreactivity is present in the Golgi complex area, as shown in the section counterstained for the Golgi complex marker GM-130. Within the Golgi complex, however, Tuba and GM-130 do not have an overlapping distribution. *B*, immunogold labeling of a lysed synaptosome demonstrating the concentration of Tuba at the periphery of the synaptic vesicle cluster in the presynaptic compartment. The *arrow* points to a clathrin-coated vesicle.

Gold immunolabeling was detected in the presynaptic compartment, where it was primarily concentrated at the periphery of synaptic vesicle clusters (Fig. 3*B*). These are the regions where clathrin-mediated endocytosis occurs (for example, see a clathrin-coated vesicle in Fig. 3*B*) and where presynaptic actin is concentrated. This localization is consistent with a role of Tuba in endocytosis and actin function, as proposed for other BAR domain-containing proteins. To begin elucidating the physiological role of Tuba, the binding partners of its SH3 domains were investigated.

The N Terminus of Tuba Binds Dynamin—To identify binding partners of the N-terminal SH3 domains of Tuba, a GST fusion protein comprising the four N-terminal SH3 domains (SH3-1,2,3,4) was generated and incubated with Triton X-100-solubilized rat brain extracts in affinity chromatography experiments. As shown by Coomassie Blue staining of SDS gels of the material retained by the beads, the fusion protein, but not GST alone, specifically and efficiently retained a protein of 100 kDa (Fig. 4*A*). This protein was identified as dynamin-1 by matrix-assisted laser desorption ionization time-of-flight (MALDI-TOF) spectrometry (data not shown) and immunoblotting (Fig. 4*B*). The interaction between the SH3 domains of Tuba and dynamin-1 is direct because it could be confirmed by far-Western blotting using HA-tagged SH3-1,2,3,4 as a probe (data not shown). Furthermore, dynamin (but not synaptotagmin) could be coprecipitated with Tuba from Triton X-100-solubilized rat brain extracts, demonstrating that the interaction can occur *in vivo* (Fig. 4*C*). The separate analysis of each of the four SH3 domains in affinity purification experiments revealed that all of them bound dynamin and that SH3-4 had the highest affinity for dynamin, followed by, in order of decreasing affinity, SH3-1, SH3-3, and SH3-2 (data not shown). We conclude that dynamin is the main ligand of the Tuba N-terminal region.

To better determine whether the interaction between dynamin and the N terminus of Tuba is relevant *in vivo*, we expressed HA-tagged SH3-1,2,3,4 in Chinese hamster ovary cells and determined its effect on transferrin uptake, a dynamin-dependent endocytic reaction. It was shown previously that SH3 domains that bind dynamin can function as potent inhibitors of this process, probably by titrating out dynamin (42, 43). When expressed in Chinese hamster ovary cells, SH3-1,2,3,4 had a cytosolic distribution and inhibited transferrin internalization (Fig. 4*D*), suggesting that the N terminus of Tuba can interact with dynamin *in vivo*. Cytosolic expression of the C-terminal SH3 domain (which does not bind dynamin; see below) had no effect on transferrin uptake (data not shown).

The C-terminal SH3 Domain of Tuba Binds to an Actin Regulatory Complex—We next searched for interactors of the C-terminal SH3 domains of Tuba. GST fusion proteins of SH3-5 and SH3-6 were generated and used in pull-down experiments with Triton X-100-solubilized rat brain extracts. No major in-

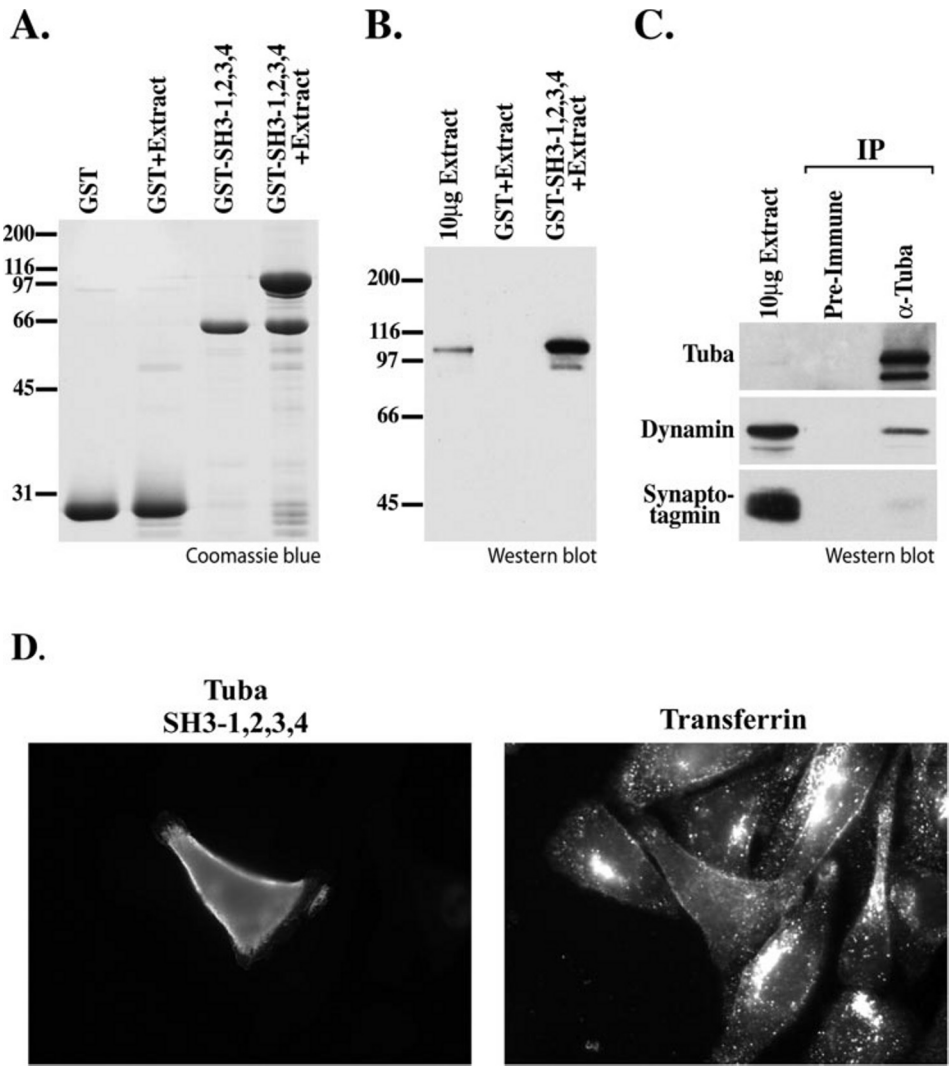

FIG. 4. **The N-terminal SH3 domains of Tuba bind dynamin-1.** *A*, bead-immobilized GST and a GST fusion protein of the N-terminal region of Tuba (SH3-1,2,3,4) were incubated with a Triton X-100-solubilized rat brain extract, and the bound material was analyzed by SDS-PAGE and Coomassie Blue staining. A band of 100 kDa (dynamin) was selectively affinity-purified. The greater abundance of dynamin than of the fusion protein used as bait is likely to reflect the oligomerization state of dynamin. *B*, shown is an anti-dynamin Western blot of the material affinity-purified by GST or the GST fusion protein. *C*, control or anti-Tuba antibodies were used to generate immunoprecipitates from a Triton X-100-solubilized rat brain extract. Western blots for Tuba, dynamin, and synaptotagmin of the immunoprecipitates are shown. *D*, Chinese hamster ovary cells were transfected with HA-tagged Tuba SH3-1,2,3,4 and then incubated for 7 min with Alexa-transferrin prior to fixation in 4% formaldehyde, followed by anti-HA immunofluorescence. Overexpression of Tuba SH3-1,2,3,4 inhibited transferrin uptake, as demonstrated by the lack of intracellular transferrin fluorescence in the transfected cell.

teractors were found for SH3-5 (data not shown). However, SH3-6 (but not GST alone) pulled down a variety of proteins as revealed by the Coomassie Blue-stained SDS gel of the affinity-purified material (Fig. 5*A*). Each of the major protein bands was excised, trypsin-digested, and analyzed by MALDI-TOF spectrometry. The identified proteins are listed in Fig. 5*A* (*upper panel*). For some proteins, the interaction was validated further by Western blotting (Fig. 5*A*, *lower panels*) (data not shown). Two of the major bands were actin and tubulin. Another was Hsp70, which is often found in eluates of pull-down experiments, possibly reflecting the promiscuous role of this ATPase in protein folding reactions. All other bands represent proteins that are either directly or indirectly linked to the regulation of actin dynamics.

The most abundant protein was N-WASP, the ubiquitous and brain enriched homolog of the Wiskott-Aldrich syndrome protein WASP (44). CR16 and WIRE (also known as WICH) are both related to WIP, a proline-rich protein that binds to actin and interacts with the N-terminal WASP-homology 1 (WH1) domain of N-WASP (45–48). WAVE1 is a neuron-specific SCAR/WAVE protein and a member of the WASP superfamily (49) that, like N-WASP, regulates actin assembly through binding and activation of the Arp2/3 complex (50). Unlike N-WASP, isolated WAVE1 is constitutively active (50), but is kept in an inhibited state while bound to a protein complex that includes PIR121 and NAP1 (51), two proteins present in the affinity-purified material. Mena, an Ena/VASP protein (30), and Lamellipodin, a novel Ena/VASP-associated protein,[3] were also present in the affinity-purified material, as was drebrin, an F-actin-binding protein (52).

Given the large number of proteins present in the affinity-purified complex, we investigated whether the occurrence of these interactions in cells was supported by immunoprecipitation experiments. When Tuba was immunoprecipitated from embryonic day 15 lysates, Mena was found to coprecipitate (Fig. 5*B*). Longer exposures revealed that the 140-kDa Mena$^+$, a neuron-specific isoform of Mena (30), was also coprecipitated.

[3] M. Krause and F. B. Gertler, unpublished data.

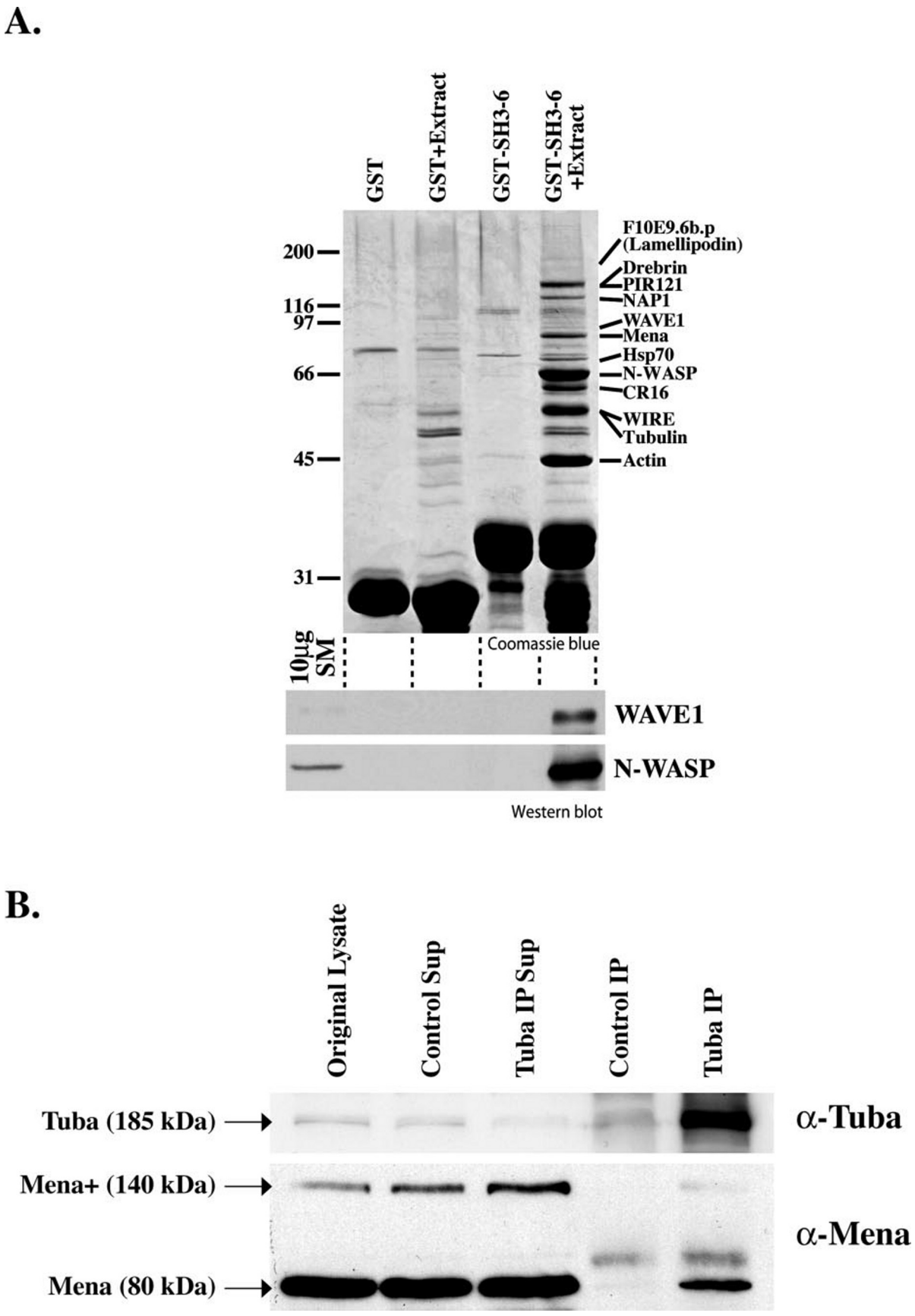

FIG. 5. **The C-terminal SH3 domain (SH3-6) of Tuba binds actin regulatory proteins.** *A*, bead-immobilized GST and a GST fusion protein of SH3-6 were incubated with a Triton X-100-solubilized rat brain extract, and the bound material was analyzed by SDS-PAGE and Coomassie Blue staining (*upper panel*). The identities of the proteins were determined by MALDI-TOF and Q-TOF mass spectrometric analysis. Binding of WAVE1 and N-WASP was confirmed by Western blot analysis (*lower panels*). *B*, control or affinity-purified anti-Tuba antibodies were used for immunoprecipitation (*IP*) from embryonic day 16 mouse lysates. The *upper panel* is a Western blot for Tuba; the *lower panel* is a Western blot for Mena. *Sup*, supernatant. *SM*, starting material.

N-WASP as well was found in the precipitated material (data not shown). These results indicate that Tuba interacts with one or more actin regulatory proteins *in vivo*.

Because the C terminus of mouse Tuba was identified as a binding partner of EVL in a yeast two-hybrid system (Fig. 1*A*) and the co-immunoprecipitation results demonstrated that Tuba and Mena interact *in vivo*, the Ena/VASP interaction was further characterized. Pull-down experiments with lysates prepared from Ena/VASP-deficient cells (referred to as D7 cells (34)) stably infected and sorted for equal expression of enhanced green fluorescent protein (EGFP) fusions of Mena, EVL, or VASP showed that the SH3-6 domain of Tuba bound to each of the three proteins, but more robustly to EVL and Mena (Fig. 6*A*). No binding was observed in cells expressing a mutant form of Mena that lacks the proline-rich region (Fig. 6*A*), indicating that this region, present in all Ena/VASP proteins, is essential for binding.

The two-hybrid results suggest that EVL and, by analogy, all Ena/VASP proteins bind to the SH3-6 domain of Tuba directly. To test this further, lysates from D7 cells and D7 cells expressing EGFP-Mena were blotted and overlaid with ^{32}P-labeled GST-SH3-6. A band at ~115 kDa (the expected size of EGFP-Mena) was observed only in the lysate from D7 cells expressing EGFP-Mena (Fig. 6*B*, *D7 E-M*). GST-SH3-6 pull-down experiments with the same lysates were performed, and the affinity-purified material from these pull-down experiments was blotted and overlaid with ^{32}P-labeled GST-SH3-6. Again, SH3-6 bound directly to a band with the predicted molecular mass of EGFP-Mena only in cell lysates expressing EGFP-Mena (Fig. 6*B*). Thus, Tuba binds directly to Ena/VASP proteins, consistent with the initial two-hybrid results. A direct interaction between SH3-6 and other proteins present in the affinity-purified material was also observed (Fig. 6*B*). One prominent band had the predicted electrophoretic mobility of N-WASP, and Western blotting suggested that this band was indeed N-WASP (data not shown). The identity of a major band just above N-WASP remains unknown, but we speculate that it might be a member of the WIP family of proteins. Interestingly, the intensity of this band decreased in cells expressing EGFP-Mena, possibly due to competition between Mena and this protein binding to SH3-6.

A gel overlay with ^{32}P-labeled GST-SH3-6 was also performed on the material affinity-purified by SH3-6 from mouse brain lysate. Two prominent bands bound by SH3-6 were adjacent to the 66-kDa marker (Fig. 6*C*). Western blotting demonstrated that the upper band precisely comigrated with N-WASP (data not shown), whereas the lower band appears to be CR16 (Fig. 6*C*). The overlay experiment also revealed a prominent band at ~50 kDa and a somewhat weaker signal at ~140 kDa. Western blotting indicated that the band at 140 kDa corresponds to Mena$^+$ (Fig. 6*C*). The identity of the 50-kDa band remains unknown.

Because both Mena and N-WASP appear to bind directly to the SH3-6 domain of Tuba, we sought to map the binding site(s) within these proteins. A series of overlapping peptides corresponding to the proline-rich regions of N-WASP, WAVE1, EVL, and Mena were synthesized by the SPOTs method (53). This peptide blot was overlaid with ^{32}P-labeled GST-SH3-6 (Fig. 7*A*), and the resulting signal intensity at each peptide spot was measured and compared with the background level (Fig. 7*B*). N-WASP has two potential binding sites for SH3-6 (where the signal level was at least 6-fold over the background level), whereas EVL and Mena each have one. Strong binding to any peptide in WAVE1 was not observed. The four peptides demonstrating the strongest binding are listed in Fig. 7*C*. These results provide further evidence for direct and specific binding between SH3-6 and N-WASP and Ena/VASP proteins.

The C-terminal SH3 Domain of Tuba Can Promote F-actin Recruitment—Because the Tuba SH3-6 domain can bind to a number of actin regulatory proteins, we wondered whether concentrating this domain on a surface within the cell would result in recruitment or nucleation of F-actin. To accomplish this, we fused the SH3-6 domain to a mitochondrial anchoring sequence (SH3-6-mito), a method that has been used successfully to map protein domains that induce actin recruitment within living cells (25, 54). Because Tuba is expressed in brain and localizes to synapses, we used CAD cells, a neuron-like cell line, to express SH3-6-mito. Interestingly, in ~15–20% of transfected cells expressing high levels of SH3-6-mito, F-actin was found to co-localize with the SH3-6-mito fusion (Fig. 8, *D–F*). Therefore, overexpression of the SH3-6 domain can promote F-actin nucleation and/or recruitment within cells, presumably via one or more of the actin regulatory proteins it is known to bind *in vitro*.

The DH-BAR Region of Tuba Catalyzes the Formation of Active Cdc42—The results described above indicate that the C-terminal SH3 domain of Tuba can promote actin nucleation and/or recruitment. The presence of a DH domain in Tuba, a protein module involved in the activation of Rho family GTPases, suggests a further link to the actin cytoskeleton. The function of this domain was investigated.

Like other GTPases, Rho family GTPases cycle between a GTP-bound active state and a GDP-bound inactive state. DH domains form the core catalytic domains of enzymes that activate Rho family GTPases by catalyzing the exchange of GDP for GTP (55). We studied the substrate specificity of the DH domain of Tuba by testing its guanyl nucleotide exchange activity on three major representative members of the Rho family: RhoA, Rac1, and Cdc42. A His-tagged Tuba DH domain was used in a mant-GTP-based assay, which allows the guanyl nucleotide exchange reaction to be monitored fluorometrically (36). Unfortunately, the insolubility of the BAR domain prevented us from testing the DH-BAR fragment in this assay. The DH domain of Tuba specifically catalyzed, in a concentration-dependent manner, the activation of Cdc42, but not Rho or Rac (Fig. 9). The His-tagged DH-PH domain of Vav2, a DH domain known to have a promiscuous exchange activity on Rho, Rac, and Cdc42 (56), was used as a control to demonstrate that all three GTPases used were competent for exchange (Fig. 9). The DH domain of Tuba, although specific for Cdc42, displayed relatively low activity compared with the DH-PH domain of Vav2: ~10 μM Tuba DH domain was comparable to 200 nM Vav2 DH-PH domain. DH domains without associated PH domains are generally less active than DH-PH fragments (57). Because we believe that the BAR domain of Tuba is a functional replacement for the PH domain, this absence of the BAR domain could account for the low activity.

DISCUSSION

The striking phenotype of *shibire* (dynamin) mutants of *Drosophila* (58) and the many subsequent studies demonstrating a block of endocytosis in cells harboring dynamin mutations have strongly implicated this GTPase in the fission reaction of endocytosis (10, 59, 60). There is also strong evidence from studies in living cells and in cell-free systems of a role for dynamin in the regulation of the actin cytoskeleton. For example, disruption of dynamin function impairs neurite outgrowth (an actin-dependent process) (61) and perturbs actin dynamics in a variety of cellular contexts (14, 62, 63). Dynamin is present in actin tails (17, 18), and many dynamin-binding proteins, including intersectin (19) and syndapin (64, 65), are also regulatory components of the actin cytoskeleton. This study details

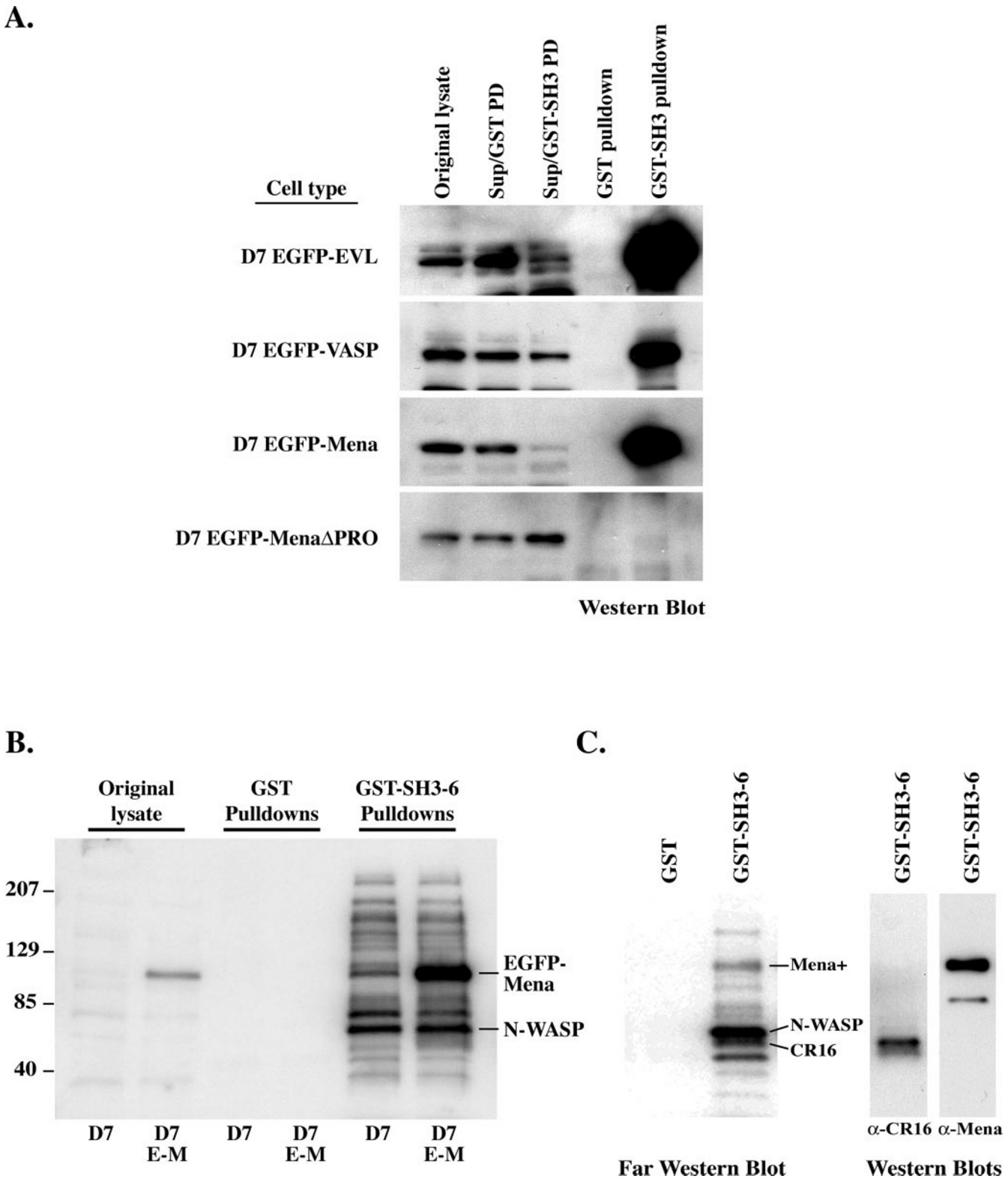

FIG. 6. **Interaction of the SH3-6 domain of Tuba with Ena/VASP proteins.** *A*, D7 cells, which contain no Ena/VASP protein family members, were infected with EGFP fusions of each member of the Ena/VASP family or of a Mena construct lacking the proline-rich domain (Δ*PRO*). Lysates from cells expressing equal levels of the fusion proteins were affinity-purified by GST or GST-SH3-6. The starting lysates, as well as the supernatant (*Sup*) and pellets of the affinity-purified material, were then processed by Western blotting with anti-EGFP antibodies. *B*, lysates of D7 cells or of D7 cells stably infected with EGFP-Mena (*D7 E-M*) were incubated with GST-SH3-6 in affinity chromatography experiments. The starting lysates and the pull-down (*PD*) products were separated by SDS-PAGE, blotted onto nitrocellulose, and overlaid with ^{32}P-labeled SH3-6. *C*, the material from mouse brain lysates affinity-purified by GST or GST-SH3-6 was separated by SDS-PAGE and overlaid with ^{32}P-labeled SH3-6 (*left panel*). The blot was stripped and reprobed with antibodies against potential ligands (*right panel*).

the discovery and characterization of a novel protein, Tuba, and its potential role as a molecular link between dynamin and actin.

The N-terminal domain of Tuba binds dynamin via multiple SH3 domains, each of which can bind independently, thus increasing the overall avidity of Tuba for this GTPase. The

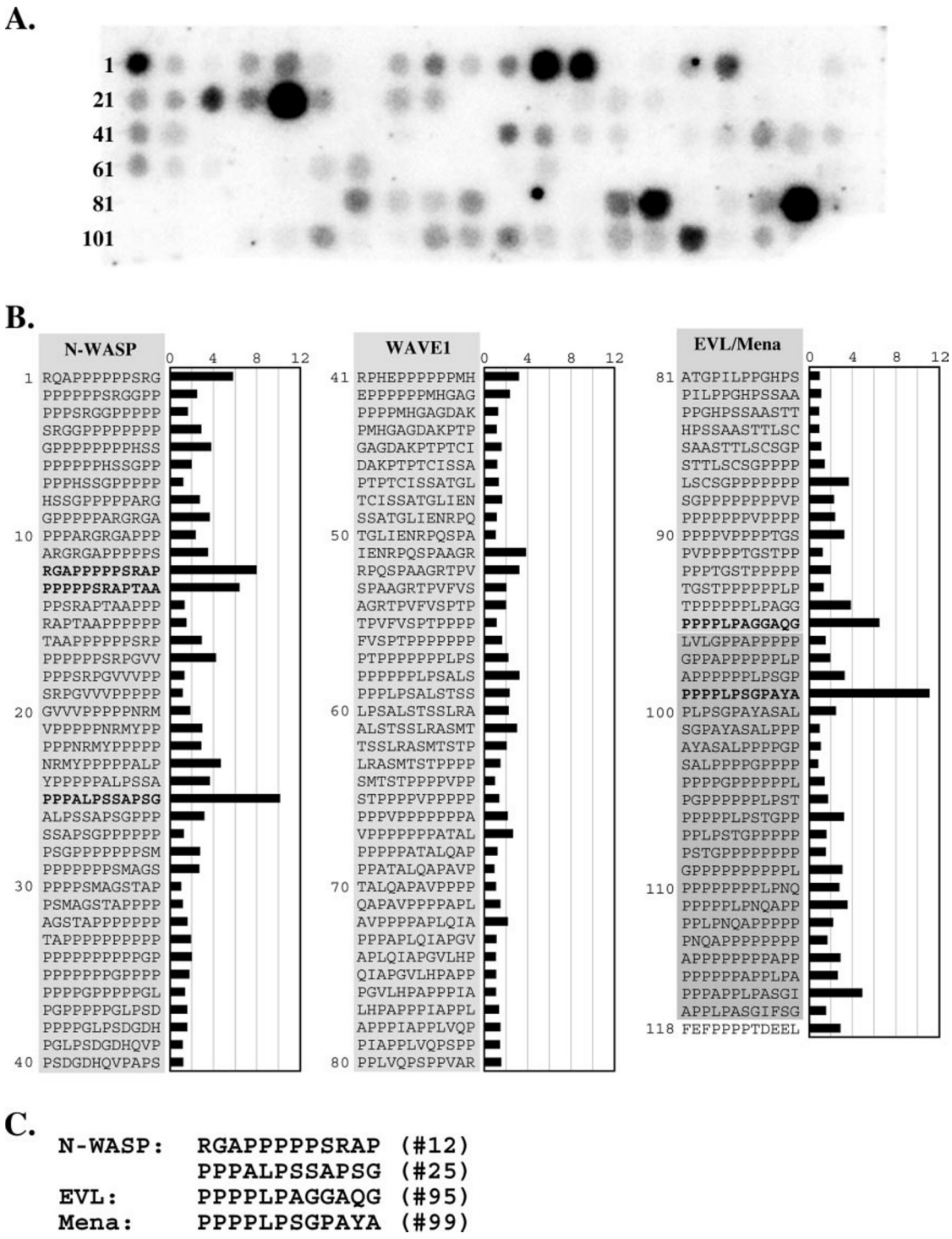

FIG. 7. **Mapping of SH3-6-binding sites.** *A*, shown is a SPOTs membrane containing an array of overlapping peptides corresponding to the proline-rich regions of N-WASP, WAVE1, EVL, and Mena overlaid with ^{32}P-labeled GST-SH3-6. *B*, individual peptide spots are listed with intensity value demonstrated graphically as value/background. Peptide 118 is a negative control proline-rich sequence that binds Ena/VASP proteins, but not SH3 domains. Peptides in which the intensity/background is >6 are in *boldface*. *C*, potential binding sites for SH3-6 in N-WASP, EVL, and Mena are listed with their corresponding peptide spot number.

interaction between Tuba and dynamin could be important for both dynamin localization and dynamin regulation, as has been shown for other SH3 domain-containing dynamin ligands (2, 4).

The C-terminal half of Tuba is linked to actin assembly via two independent mechanisms. First, the DH domain of Tuba activates Cdc42, a Rho family GTPase that binds and activates N-WASP, thereby triggering Arp2/3-mediated actin nucleation (66). Second, the C-terminal SH3 domain binds a number of key actin regulatory proteins, including Ena/VASP, N-WASP, the N-WASP-interacting protein WIRE, and CR16. Based on the effects of other SH3 domain interactors of N-WASP (19, 23), it is possible that Tuba binding activates N-WASP and that this activation may cooperate synergistically with Tuba-mediated activation of Cdc42 in promoting actin nucleation.

It is interesting to note that a Tuba isoform and Tuba relatives lack the N-terminal dynamin-binding module, suggesting that Tuba family proteins may regulate the actin cytoskeleton in processes other than endocytosis. For example, recent mod-

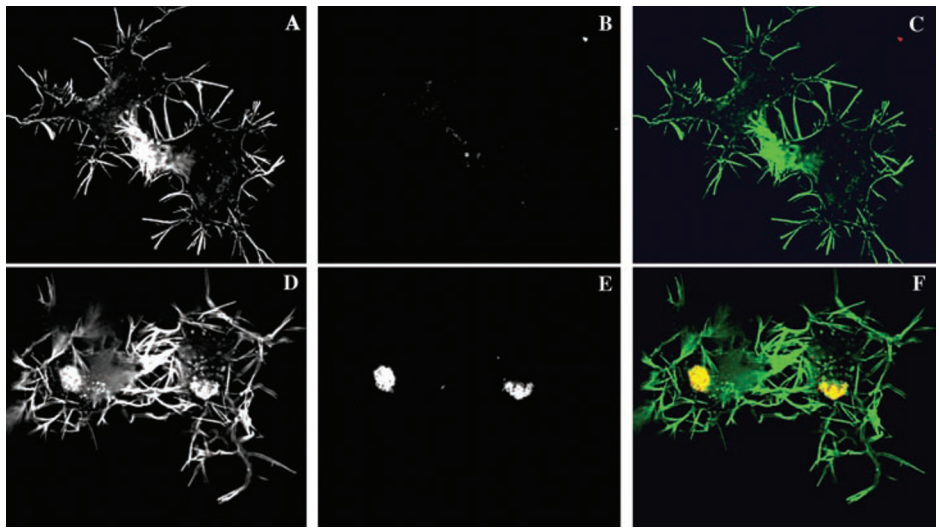

FIG. 8. **The C-terminal SH3 domain of Tuba recruits F-actin.** SH3-6-mito, a DsRed2 fusion protein of SH3-6 with a mitochondrial targeting sequence at the C terminus, was transiently transfected into CAD cells. *A–C* show control cells stained for F-actin (*A*) that lacks any notable DsRed2 signal (*B* and merge in *C*). *D–F* demonstrate the co-localization of F-actin (*D*) with SH3-6-mito (*E* and merge in *F*) in two highly expressing cells.

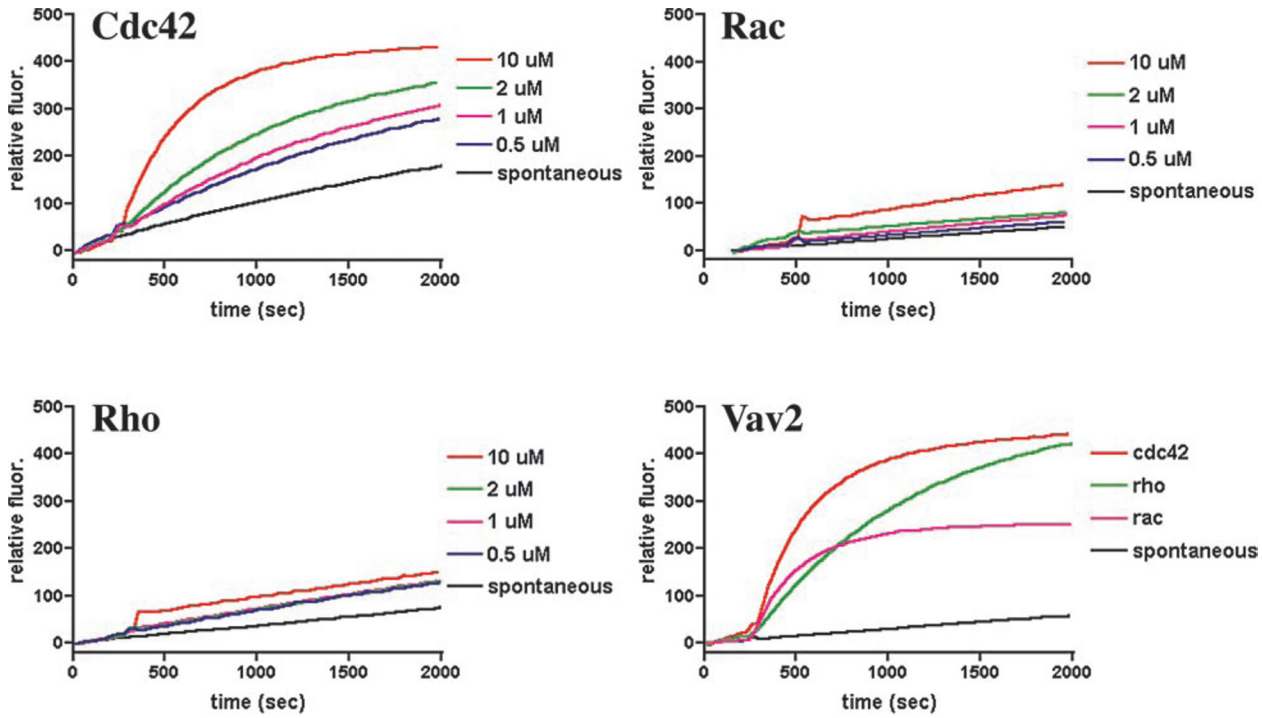

FIG. 9. **The DH domain of Tuba specifically catalyzes the activation of Cdc42.** The indicated GTPases (2 μM) were incubated with 400 nM mant-GTP for 200 s prior to addition of the indicated concentrations of His-tagged Tuba DH domain. Exchange activity was followed by the increase in fluorescence (*fluor.*), normalized to its starting value, and reflects the binding of mant-GTP to the GTPases. To verify the integrity of the GTPases, a fragment of Vav2 (0.2 μM) containing the DH and PH domains and previously shown to be active on Rho, Rac, and Cdc42 was used to load mant-GTP onto the GTPases under identical conditions.

els for filopodial formation propose that filipodia emerge from clouds of Arp2/3-generated actin nuclei by elongation of filaments that are protected from capping and subsequently bundled (67). The Tuba C-terminal SH3 domain binds to Ena/VASP proteins. Because Ena/VASP proteins function to promote actin filament elongation and have a potential role in filopodial formation (68), we speculate that Ena/VASP proteins are recruited by Tuba to promote actin filament growth after N-WASP-dependent actin nucleation. Therefore, Tuba is well positioned to promote filopodial formation by coordinating the activation of N-WASP (directly and via Cdc42) with the recruitment of Ena/VASP family members to antagonize capping protein, thus permitting filament elongation. The presence of predicted coiled-coil domains in Tuba both in the BAR domain (9, 69) and upstream of the BAR domain (Fig. 1*A*) suggests a potential multimerization of the molecule as seen for other BAR and SH3 domain-containing proteins (9, 69), thus providing a further mechanism for the functional coordination of multiple binding partners.

The material affinity-purified by this SH3-6 domain also includes the WAVE1-PIR121-NAP125 complex, which is involved in the regulation of Arp2/3-mediated actin nucleation via Rac1 (51). Interestingly GEI-18, the worm TUBA homolog, was identified in a two-hybrid screen for binding partners of GEX3, the worm NAP125 homolog (40, 70), suggesting that interactions between Tuba and the WAVE inhibitory complex are evolutionarily conserved. It will be interesting to see what role, if any, Tuba plays in Rac-mediated signaling.

The SPOTs peptide binding provided further evidence for a direct and specific interaction between SH3-6 and N-WASP and Ena/VASP proteins. Four potential proline-rich SH3-6-binding sites were identified. Interestingly, the first site in

N-WASP (RAGPPPPPSRAP, peptide 12) is very similar to a site found in the N-WASP-interacting protein WIRE (RGKPPPPPSRTP), a protein that is also found in the affinity-purified Tuba SH3-6 complex. Far-Western data suggested that SH3-6 binds directly to more than N-WASP and Mena; and given that WIRE is ~50 kDa, we believe that the smallest band in the brain far-Western blot (Fig. 5*B*) is likely WIRE. Interestingly, the second site in N-WASP and the sites in Mena and EVL all contain PP*X*LP.

The presence of binding sites for both N-WASP and dynamin, together with the presence of a Cdc42-specific DH domain, is also a characteristic of intersectin (19). However, in Tuba, the dynamin- and actin cytoskeleton-binding domains are segregated at opposite ends of the protein. In intersectin, an intramolecular regulatory mechanism has been demonstrated showing that the binding of N-WASP stimulates the DH domain to activate Cdc42, thus resulting in a synergistic activation of Arp2/3-mediated actin nucleation (19). The poor solubility of recombinant Tuba has prevented us from testing whether N-WASP binding can stimulate nucleotide exchange activity. The presence of putative consensus sites for SH3 domain binding in Tuba raises the possibility that inhibitory intramolecular SH3 domain-mediated interactions may occur (71). These interactions might be released by the binding of appropriate SH3 domain ligands.

An additional unique feature of the Tuba family is the presence of a BAR domain, rather than a PH domain, downstream of a DH domain. This is an exception to a nearly absolute rule (32, 55). PH domains bind phosphoinositides (72), and their interaction with lipids in the bilayer recruits catalytic DH domains to their sites of action. In some cases, PH domains also have a direct regulatory role, such that PH domain binding to the membrane results in stimulation of exchange activity from the DH domain (32). As mentioned before, the absence of the BAR domain in the DH domain of Tuba used for guanyl nucleotide exchange factor assays could account for its low activity. Other BAR domains bind lipid bilayers (8, 10). Given poor solubility, we could not reliably test the lipid-binding properties of the BAR domain of Tuba, although preliminary experiments support this possibility.[4] Thus, the BAR domain of Tuba may functionally replace a PH domain. It is worth noting that many BAR domain-containing proteins such as Tuba can bind dynamin and often contain modules associated with the actin cytoskeleton,[2] suggesting an evolutionary relationship (5, 6).

The precise role of Tuba in cell and synaptic physiology remains to be defined. The properties of this protein reinforce the hypothesis that the functions of dynamin and actin are strongly interrelated, although we still do not yet understand precisely how. Two major possibilities remain open. The first is that dynamin has a primary function in endocytosis and that its connection to actin may reflect the need to coordinate the endocytic reaction with rearrangements of the actin cytoskeleton surrounding endocytic sites. These rearrangements may be needed to allow budding and fission or to propel the newly formed endocytic vesicles via actin tails. The second is that dynamin functions to regulate the actin cytoskeleton and that the powerful effect of mutant dynamin on endocytosis reflects the critical role of actin in the endocytic reaction.

Acknowledgment—Protein and DNA analysis and oligonucleotide synthesis were performed in the Yale Howard Hughes Medical Institute Biopolymer-Keck Foundation Biotechnology Resource Laboratory.

REFERENCES

1. Conner, S. D., and Schmid, S. L. (2003) *Nature* **422,** 37–44
2. Slepnev, V. I., and De Camilli, P. (2000) *Nat. Rev. Neurosci.* **1,** 161–172
3. Hinshaw, J. E. (2000) *Annu. Rev. Cell Dev. Biol.* **16,** 483–519
4. Gout, I., Dhand, R., Hiles, I. D., Fry, M. J., Panayotou, G., Das, P., Truong, O., Totty, N. F., Hsuan, J., Booker, G. W., Campbell, I. D., and Waterfield, M. D. (1993) *Cell* **75,** 25–36
5. David, C., McPherson, P. S., Mundigl, O., and De Camilli, P. (1996) *Proc. Natl. Acad. Sci. U. S. A.* **93,** 331–335
6. Ringstad, N., Nemoto, Y., and De Camilli, P. (1997) *Proc. Natl. Acad. Sci. U. S. A.* **94,** 8569–8574
7. Ramjaun, A. R., Micheva, K. D., Bouchelet, I., and McPherson, P. S. (1997) *J. Biol. Chem.* **272,** 16700–16706
8. Farsad, K., Ringstad, N., Takei, K., Floyd, S. R., Rose, K., and De Camilli, P. (2001) *J. Cell Biol.* **155,** 193–200
9. Wigge, P., Kohler, K., Vallis, Y., Doyle, C. A., Owen, D., Hunt, S. P., and McMahon, H. T. (1997) *Mol. Biol. Cell* **8,** 2003–2015
10. Takei, K., Slepnev, V. I., Haucke, V., and De Camilli, P. (1999) *Nat. Cell Biol.* **1,** 33–39
11. Lombardi, R., and Riezman, H. (2001) *J. Biol. Chem.* **276,** 6016–6022
12. Munn, A. L. (2001) *Biochim. Biophys. Acta* **1535,** 236–257
13. Qualmann, B., Kessels, M. M., and Kelly, R. B. (2000) *J. Cell Biol.* **150,** F111–F116
14. Schafer, D. A. (2002) *Curr. Opin. Cell Biol.* **14,** 76–81
15. Merrifield, C. J., Feldman, M. E., Wan, L., and Almers, W. (2002) *Nat. Cell Biol.* **4,** 691–698
16. Merrifield, C. J., Moss, S. E., Ballestrem, C., Imhof, B. A., Giese, G., Wunderlich, I., and Almers, W. (1999) *Nat. Cell Biol.* **1,** 72–74
17. Lee, E., and De Camilli, P. (2002) *Proc. Natl. Acad. Sci. U. S. A.* **99,** 161–166
18. Orth, J. D., Krueger, E. W., Cao, H., and McNiven, M. A. (2002) *Proc. Natl. Acad. Sci. U. S. A.* **99,** 167–172
19. Hussain, N. K., Jenna, S., Glogauer, M., Quinn, C. C., Wasiak, S., Guipponi, M., Antonarakis, S. E., Kay, B. K., Stossel, T. P., Lamarche-Vane, N., and McPherson, P. S. (2001) *Nat. Cell Biol.* **3,** 927–932
20. Roos, J., and Kelly, R. B. (1998) *J. Biol. Chem.* **273,** 19108–19119
21. Mullins, R. D. (2000) *Curr. Opin. Cell Biol.* **12,** 91–96
22. Rohatgi, R., Ho, H. Y., and Kirschner, M. W. (2000) *J. Cell Biol.* **150,** 1299–1310
23. Rohatgi, R., Nollau, P., Ho, H. Y., Kirschner, M. W., and Mayer, B. J. (2001) *J. Biol. Chem.* **276,** 26448–26452
24. Higgs, H. N., and Pollard, T. D. (2000) *J. Cell Biol.* **150,** 1311–1320
25. Kessels, M. M., and Qualmann, B. (2002) *EMBO J.* **21,** 6083–6094
26. Welch, M. D., Rosenblatt, J., Skoble, J., Portnoy, D. A., and Mitchison, T. J. (1998) *Science* **281,** 105–108
27. Laurent, V., Loisel, T. P., Harbeck, B., Wehman, A., Grobe, L., Jockusch, B. M., Wehland, J., Gertler, F. B., and Carlier, M. F. (1999) *J. Cell Biol.* **144,** 1245–1258
28. Geese, M., Loureiro, J. J., Bear, J. E., Wehland, J., Gertler, F. B., and Sechi, A. S. (2002) *Mol. Biol. Cell* **13,** 2383–2396
29. Bear, J. E., Svitkina, T. M., Krause, M., Schafer, D. A., Loureiro, J. J., Strasser, G. A., Maly, I. V., Chaga, O. Y., Cooper, J. A., Borisy, G. G., and Gertler, F. B. (2002) *Cell* **109,** 509–521
30. Gertler, F. B., Niebuhr, K., Reinhard, M., Wehland, J., and Soriano, P. (1996) *Cell* **87,** 227–239
31. Kwiatkowski, A. V., Gertler, F. B., and Loureiro, J. J. (2003) *Trends Cell Biol.* **13,** 386–392
32. Rossman, K. L., Cheng, L., Mahon, G. M., Rojas, R. J., Snyder, J. T., Whitehead, I. P., and Sondek, J. (2003) *J. Biol. Chem.* **278,** 18393–18400
33. Floyd, S. R., Porro, E. B., Slepnev, V. I., Ochoa, G. C., Tsai, L. H., and De Camilli, P. (2001) *J. Biol. Chem.* **276,** 8104–8110
34. Bear, J. E., Loureiro, J. J., Libova, I., Fassler, R., Wehland, J., and Gertler, F. B. (2000) *Cell* **101,** 717–728
35. De Camilli, P., Harris, S. M., Jr., Huttner, W. B., and Greengard, P. (1983) *J. Cell Biol.* **96,** 1355–1373
36. Snyder, J. T., Worthylake, D. K., Rossman, K. L., Betts, L., Pruitt, W. M., Siderovski, D. P., Der, C. J., and Sondek, J. (2002) *Nat. Struct. Biol.* **9,** 468–475
37. Pistor, S., Chakraborty, T., Niebuhr, K., Domann, E., and Wehland, J. (1994) *EMBO J.* **13,** 758–763
38. McPherson, P. S., Garcia, E. P., Slepnev, V. I., David, C., Zhang, X., Grabs, D., Sossin, W. S., Bauerfeind, R., Nemoto, Y., and De Camilli, P. (1996) *Nature* **379,** 353–357
39. Cases-Langhoff, C., Voss, B., Garner, A. M., Appeltauer, U., Takei, K., Kindler, S., Veh, R. W., De Camilli, P., Gundelfinger, E. D., and Garner, C. C. (1996) *Eur. J. Cell Biol.* **69,** 214–223
40. Tsuboi, D., Qadota, H., Kasuya, K., Amano, M., and Kaibuchi, K. (2002) *Biochem. Biophys. Res. Commun.* **292,** 697–701
41. Nakamura, N., Rabouille, C., Watson, R., Nilsson, T., Hui, N., Slusarewicz, P., Kreis, T. E., and Warren, G. (1995) *J. Cell Biol.* **131,** 1715–1726
42. Shupliakov, O., Low, P., Grabs, D., Gad, H., Chen, H., David, C., Takei, K., De Camilli, P., and Brodin, L. (1997) *Science* **276,** 259–263
43. Wigge, P., Vallis, Y., and McMahon, H. T. (1997) *Curr. Biol.* **7,** 554–560
44. Miki, H., Miura, K., and Takenawa, T. (1996) *EMBO J.* **15,** 5326–5335
45. Kato, M., Miki, H., Kurita, S., Endo, T., Nakagawa, H., Miyamoto, S., and Takenawa, T. (2002) *Biochem. Biophys. Res. Commun.* **291,** 41–47
46. Aspenstrom, P. (2002) *Exp. Cell Res.* **279,** 21–33
47. Ho, H. Y., Rohatgi, R., Ma, L., and Kirschner, M. W. (2001) *Proc. Natl. Acad. Sci. U. S. A.* **98,** 11306–11311
48. Martinez-Quiles, N., Rohatgi, R., Anton, I. M., Medina, M., Saville, S. P., Miki, H., Yamaguchi, H., Takenawa, T., Hartwig, J. H., Geha, R. S., and Ramesh, N. (2001) *Nat. Cell Biol.* **3,** 484–491
49. Miki, H., Suetsugu, S., and Takenawa, T. (1998) *EMBO J.* **17,** 6932–6941
50. Machesky, L. M., Mullins, R. D., Higgs, H. N., Kaiser, D. A., Blanchoin, L., May, R. C., Hall, M. E., and Pollard, T. D. (1999) *Proc. Natl. Acad. Sci. U. S. A.* **96,** 3739–3744
51. Eden, S., Rohatgi, R., Podtelejnikov, A. V., Mann, M., and Kirschner, M. W.

[4] M. A. Salazar and P. De Camilli, unpublished data.

(2002) *Nature* **418,** 790–793
52. Ishikawa, R., Hayashi, K., Shirao, T., Xue, Y., Takagi, T., Sasaki, Y., and Kohama, K. (1994) *J. Biol. Chem.* **269,** 29928–29933
53. Frank, R. (2002) *J. Immunol. Methods* **267,** 13–26
54. Pistor, S., Chakraborty, T., Walter, U., and Wehland, J. (1995) *Curr. Biol.* **5,** 517–525
55. Hoffman, G. R., and Cerione, R. A. (2002) *FEBS Lett.* **513,** 85–91
56. Liu, B. P., and Burridge, K. (2000) *Mol. Cell. Biol.* **20,** 7160–7169
57. Whitehead, I. P., Campbell, S., Rossman, K. L., and Der, C. J. (1997) *Biochim. Biophys. Acta* **1332,** F1–F23
58. Koenig, J. H., and Ikeda, K. (1989) *J. Neurosci.* **9,** 3844–3860
59. Hinshaw, J. E., and Schmid, S. L. (1995) *Nature* **374,** 190–192
60. Marks, B., Stowell, M. H., Vallis, Y., Mills, I. G., Gibson, A., Hopkins, C. R., and McMahon, H. T. (2001) *Nature* **410,** 231–235
61. Masur, S. K., Kim, Y. T., and Wu, C. F. (1990) *J. Neurogenet.* **6,** 191–206
62. Krueger, E. W., Orth, J. D., Cao, H., and McNiven, M. A. (2003) *Mol. Biol. Cell* **14,** 1085–1096
63. Ochoa, G. C., Slepnev, V. I., Neff, L., Ringstad, N., Takei, K., Daniell, L., Kim, W., Cao, H., McNiven, M., Baron, R., and De Camilli, P. (2000) *J. Cell Biol.* **150,** 377–389
64. Qualmann, B., and Kelly, R. B. (2000) *J. Cell Biol.* **148,** 1047–1062
65. Modregger, J., Ritter, B., Witter, B., Paulsson, M., and Plomann, M. (2000) *J. Cell Sci.* **113,** 4511–4521
66. Rohatgi, R., Ma, L., Miki, H., Lopez, M., Kirchhausen, T., Takenawa, T., and Kirschner, M. W. (1999) *Cell* **97,** 221–231
67. Vignjevic, D., Yarar, D., Welch, M. D., Peloquin, J., Svitkina, T., and Borisy, G. G. (2003) *J. Cell Biol.* **160,** 951–962
68. Svitkina, T. M., Bulanova, E. A., Chaga, O. Y., Vignjevic, D. M., Kojima, S., Vasiliev, J. M., and Borisy, G. G. (2003) *J. Cell Biol.* **160,** 409–421
69. Ringstad, N., Nemoto, Y., and De Camilli, P. (2001) *J. Biol. Chem.* **276,** 40424–40430
70. Soto, M. C., Qadota, H., Kasuya, K., Inoue, M., Tsuboi, D., Mello, C. C., and Kaibuchi, K. (2002) *Genes Dev.* **16,** 620–632
71. Zamanian, J. L., and Kelly, R. B. (2003) *Mol. Biol. Cell* **14,** 1624–1637
72. Lemmon, M. A., Ferguson, K. M., and Abrams, C. S. (2002) *FEBS Lett.* **513,** 71–76